Arch Appl Mech (2014) 84:1103–1115
DOI 10.1007/s00419-014-0868-4

ORIGINAL

Yang Gao · Andreas Ricoeur · Liang-Liang Zhang · Lian-Zhi Yang

Crack solutions and weight functions for plane problems in three-dimensional quasicrystals

Received: 22 December 2013 / Accepted: 1 May 2014 / Published online: 17 May 2014

Abstract The plane problems of an elliptic hole and a crack in three-dimensional quasicrystals subject to far-field loadings are studied. The generalized Stroh formalism is adopted here, and the explicit solutions for the coupled fields are obtained in the closed form. When the elliptic hole reduces to a crack, the analytical expressions for both the entire fields and the asymptotic fields near the crack tip are determined. The crack theory of quasicrystals, including the determination of the field intensity factors, crack opening displacements, crack tip energy release rates and so on, is a prerequisite. Applying Betti's theorem of reciprocity, the weight functions for a quasicrystal body with a crack are derived. The weight functions provide a means of calculating the intensity factors for the crack when both phonon and phason point forces are imposed at arbitrary locations.

Keywords Three-dimensional quasicrystal · Elliptic hole · Crack · Field intensity factor · Energy release rate · Crack weight function

1 Introduction

Quasicrystals (QCs) possess an aperiodic but ordered structure and have to be classified in-between crystals and glasses. They are of considerable interest within an engineering context due to their advantageous properties. Among those, the low friction coefficient, low adhesion, high wear resistance and low level of porosity should be mentioned. Thus, QCs have become the focus of theoretical and experimental studies in the physics of condensed matter since the first discovery of the icosahedral QC in Al–Mn alloys [17,31]. The physical properties of QCs have been the subject of numerous studies of solid-state physicists and materials scientists ever since. Among them, the experimental research and theoretical analyses on elasticity and defects have made great progress [1,26,27,40]. In particular, the field of linear elastic theory of QCs has been investigated for many years [5,13,16,32]. The progress in mechanics involving the theory of elasticity and defects has been written down in review articles for detail [7,12].

Because of the intrinsic brittleness of QC materials, cracks play an important role by drastically reducing the fracture strength and fatigue limits. Recently, some experimental results have been reported where two-dimensional (2D) defects such as planar defects and cracks produced by cleavage have been detected in QCs [4,6]. Thus, macroscopic cracks inevitably exist in QC solids, and their propagation is the basic cause of

Y. Gao (✉) · L.-L. Zhang · L.-Z. Yang
College of Science, China Agricultural University, Beijing 100083, People's Republic of China
E-mail: gaoyangg@gmail.com

A. Ricoeur
Institute of Mechanics, University of Kassel, 34125 Kassel, Germany

L.-L. Zhang · L.-Z. Yang
College of Engineering, China Agricultural University, Beijing 100083, People's Republic of China

material failure. However, the theory and criteria of fracture mechanics of QCs are fundamentally different from those in conventional linear elastic solids. This fact is due to the introduction of the phason field resulting in significant discrepancies, e.g., between Hooke's law in classical linear elastic theory and that in QC linear elastic theory or between the elastic energy density in conventional and QC linear elastic theory.

A Griffith crack embedded in a decagonal QC subjected to a remote uniform tension has been studied by using the Fourier transform [19,20,41]. A circular crack problem in three-dimensional (3D) icosahedral QCs was investigated by using the perturbation method [28]. The elastic analysis of a Mode II (in-plane shear) crack penetrating through an icosahedral QC was made with the aid of the displacement potential functions [42]. By using the general solution of 2D hexagonal QCs [10], a penny-shaped crack problem under axisymmetric loading and shear loading in the material is investigated [8]. By means of a general method of holomorphic vector functions in 1D QCs [11], the intensity factors of phonon and phason fields were determined, and the physical meaning of the results relative to phason and the difference between crack problems in crystals and QCs were figured out. By using the generalized Lekhnitskii formalism combined with the analytical continuation principle of [9,24] investigated the plane problem of an elliptic hole or crack in a cubic QC solid subjected to uniform loading.

Extension of the conventional linear elastic fracture mechanics to QCs will be helpful to gain basic understanding of how the mechanical properties of QCs are influenced by the presence of cracks. We analyze the generalized 2D problem of an infinite 3D QC medium with an elliptic hole and a crack by using the generalized Stroh formalism. The general solutions for a medium subjected to remote uniform loadings are presented in explicit and closed form. When the hole degenerates into a crack, more concise results for both the entire fields and the asymptotic fields near the crack tip are obtained. The fracture quantities of QCs, i.e., field intensity factors, crack opening displacements, energy release rates and so on, are a prerequisite. Moreover, the crack weight functions are derived and applied to calculate field intensity factors in a cracked body due to both phonon and phason point forces at arbitrary locations.

2 Basic equations of 3D QCs

If the atomic arrangement is quasiperiodic in all the three directions [33], where phonon and phason fields exist simultaneously, then the solid is a 3D QC, such as an icosahedral QC [31] and a cubic QC [26]. According to the cut-and-projection method, a 3D quasilattice can be obtained by selected projection of the respective 6D periodical lattice [18,27], with a huge number of field variables and field equations involving elasticity.

The elastic displacement fields of QCs are divided into two parts: the phonon field u_i in physical space $E^{\parallel}$ and the phason field w_i in the complementary orthogonal space $E^{\perp}$. Within the framework of the elastic theory of QCs [21], both the phonon and the phason are coupled with each other and are considered as continuous medium field variables. u_i is analogous to the displacement field of usual crystals. The elementary excitation associated with the phonon mode is propagating. The gradient of u_i describes the change in shape and volume of the unit cells. The introduction of the phason gives a macro-description of the quasiperiodicity of the new solid phase. w_i is diffusive due to the elementary excitation associated with the phason mode. Moreover, the phason phase characterizes the degree of freedom associated with relative translation of incommensurate sub-lattices, or equivalently, with special atomic rearrangements. The gradient of w_i describes the local rearrangements of the unit cells. Corresponding to the phonon and phason parameters, there are two stress fields σ_{ij} and H_{ij} associated with two strain fields ε_{ij} and w_{ij}, respectively, the latter being a new parameter in QC elasticity which is asymmetric for most classes of QCs except the cubic QCs.

Ding et al. [5] proposed a generalized elastic theory and obtained a generalized Hooke's law and the equilibrium equation for QCs. In a fixed rectangular coordinate system x_i, the following equations describe the linear constitutive behavior of QCs, i.e., the generalized Hooke's law is expressed as

$$\sigma_{ij} = C_{ijkl}\varepsilon_{kl} + R_{ijkl}w_{kl},\ H_{ij} = R_{klij}\varepsilon_{kl} + K_{ijkl}w_{kl}. \tag{1}$$

In the following formulation, lower case Latin subscripts will always range from 1 to 3, and upper case Latin subscripts will range from 1 to 6, with summation over repeated subscripts implied. C_{ijkl} and K_{ijkl} denote elastic constants in the phonon and phason fields, respectively, R_{ijkl} phonon–phason coupling elastic constants. Moreover, they satisfy the symmetric properties

$$C_{ijkl} = C_{klij} = C_{jikl} = C_{ijlk},\ K_{ijkl} = K_{klij},\ R_{ijkl} = R_{jikl}. \tag{2}$$

The positivity of the elastic strain energy density requires that the elastic tensors C_{ijkl} and K_{ijkl} must be positive definite. Namely, when the strain tensors ε_{ij} and w_{ij} are entirely nonzero, they satisfy the conditions

$$C_{ijkl}\varepsilon_{ij}\varepsilon_{kl} > 0,\ K_{ijkl}w_{ij}w_{kl} > 0. \tag{3}$$

In infinitesimal deformation setting, the strain fields are derived from displacement gradients:

$$\varepsilon_{ij} = \left(u_{i,j} + u_{j,i}\right)/2,\ w_{ij} = w_{i,j}, \tag{4}$$

where a comma stands for differentiation with respect to the spatial coordinate. The static equilibrium equations in the absence of body forces are [21]

$$\sigma_{ij,j} = 0,\ H_{ij,j} = 0. \tag{5}$$

Following ideas for piezoelectrics [38,39] and piezoelectric–piezomagnetic media [3,36], the basic equations (1) and (5) can be combined into one equation, respectively. A 6D generalized displacement vector is constructed

$$u_I = u_I\ (I = 1, 2, 3);\ u_I = w_{I-3}\ (I = 4, 5, 6), \tag{6}$$

and a 6×3 generalized stress tensor

$$\sigma_{Ij} = \sigma_{Ij}\ (I = 1, 2, 3);\ \sigma_{Ij} = H_{(I-3)j}\ (I = 4, 5, 6), \tag{7}$$

where the phonon and phason fields are collected in a compact form. Next, the definition of the elastic stiffness tensor is extended according to

$$\begin{aligned} &E_{IjKl} = C_{IjKl}\ (I, K = 1, 2, 3);\ E_{IjKl} = R_{Ij(K-3)l}\ (I = 1, 2, 3; K = 4, 5, 6);\\ &E_{IjKl} = R_{Kl(I-3)j}\ (I = 4, 5, 6; K = 1, 2, 3);\ E_{IjKl} = K_{(I-3)j(K-3)l}\ (I, K = 4, 5, 6). \end{aligned} \tag{8}$$

The basic Equations (1) and (5) can now be rewritten in an expanded tensor notation as

$$\sigma_{Ij} = E_{IjKl}\,u_{K,l}, \tag{9}$$

$$\sigma_{Ij,j} = 0. \tag{10}$$

3 Generalization of the Stroh formalism for 3D QCs

It is well known that the Stroh formalism [34,35,38] is an elegant and powerful tool to deal with 2D deformation of anisotropic elastic materials. It has been applied successfully to some areas, such as anisotropic thermoelasticity [14], piezoelectric materials [25] and 1D QCs [11] for the first time. There appears to be scarce work on the extension of the 2D Stroh formalism to full 3D elasticity problems. Barnett and Lothe [2] were the first to establish a link between the 3D solution and the 2D Stroh formalism. Ting [38] showed that the 3D Green's function for an infinite space as well as the interfacial Green's function for an infinite composite space is also connected with Barnett–Lothe tensors.

In terms of mathematical approaches, the formulation of 2D boundary value problems for 3D QCs is a straightforward extension of solutions for the anisotropic elasticity. Therefore, the generalization of the Stroh formalism for 3D QCs follows a procedure outlined by [38]. Consider a generalized 2D problem, in which all field variables are dependent on x_1 and x_2. Since derivatives with respect to x_3 disappear, the strains ε_{33} and w_{33} are zero, see Eq. (4). The static equilibrium equations (10) reduce to

$$\sigma_{I1,1} + \sigma_{I2,2} = 0. \tag{11}$$

This implies that there exists a 6D generalized stress function vector φ_I representing the components σ_{I1} and σ_{I2} as follows:

$$\sigma_{I1} = -\varphi_{I,2},\ \sigma_{I2} = \varphi_{I,1}. \tag{12}$$

Inserting Eq. (12) into the constitutive relations (9) yields a relationship between $\boldsymbol{u}$ and $\boldsymbol{\varphi}$, in matrix notation reading

$$\boldsymbol{Q}\boldsymbol{u}_{,1} + \boldsymbol{R}\boldsymbol{u}_{,2} = -\boldsymbol{\varphi}_{,2},\ \boldsymbol{R}^T\boldsymbol{u}_{,1} + \boldsymbol{T}\boldsymbol{u}_{,2} = \boldsymbol{\varphi}_{,1}, \tag{13}$$

where the superscript T stands for the transpose, and $\boldsymbol{Q}$, $\boldsymbol{R}$ and $\boldsymbol{T}$ are 6×6 real matrices with components

$$Q_{IK} = E_{I1K1},\ R_{IK} = E_{I1K2},\ T_{IK} = E_{I2K2}.$$

The matrices $\boldsymbol{Q}$ and $\boldsymbol{T}$ are symmetric but not positive definite. However, they can be shown to be nonsingular. We may combine the two equations in Eq. (13) into one equation as

$$\begin{bmatrix} \boldsymbol{Q} & 0 \\ \boldsymbol{R}^{\mathrm{T}} & -\boldsymbol{I} \end{bmatrix} \begin{bmatrix} \boldsymbol{u}_{,1} \\ \boldsymbol{\varphi}_{,1} \end{bmatrix} + \begin{bmatrix} \boldsymbol{R} & \boldsymbol{I} \\ \boldsymbol{T} & 0 \end{bmatrix} \begin{bmatrix} \boldsymbol{u}_{,2} \\ \boldsymbol{\varphi}_{,2} \end{bmatrix} = 0, \tag{14}$$

where $\boldsymbol{I}$ is the unit matrix. Equation (14) can be rewritten as

$$\boldsymbol{N} \begin{bmatrix} \boldsymbol{u}_{,1} \\ \boldsymbol{\varphi}_{,1} \end{bmatrix} = \begin{bmatrix} \boldsymbol{u}_{,2} \\ \boldsymbol{\varphi}_{,2} \end{bmatrix}, \tag{15}$$

where $\boldsymbol{N}$ is a 12×12 block matrix,

$$\boldsymbol{N} = \begin{bmatrix} \boldsymbol{N}_1 & \boldsymbol{N}_2 \\ \boldsymbol{N}_3 & \boldsymbol{N}_1^{\mathrm{T}} \end{bmatrix}, \ \boldsymbol{N}_1 = -\boldsymbol{T}^{-1}\boldsymbol{R}^{\mathrm{T}}, \ \boldsymbol{N}_2 = \boldsymbol{T}^{-1}, \ \boldsymbol{N}_3 = \boldsymbol{R}\boldsymbol{T}^{-1}\boldsymbol{R}^{\mathrm{T}} - \boldsymbol{Q}. \tag{16}$$

The real 6×6 matrices $\boldsymbol{N}_2$ and $\boldsymbol{N}_3$ are symmetric. As noted first by [29], the derivation of Eq. (15) does not invoke homogeneity, and hence, Eq. (15) applies to inhomogeneous materials as well.

If the material is homogeneous, the Stroh formalism for elastic or piezoelectric solids [22,23] can be extended to QC solids. Thus, the general solution of Eq. (15) is adopted as

$$\boldsymbol{u} = \boldsymbol{a} f(z), \ \boldsymbol{\varphi} = \boldsymbol{b} f(z), \ z = x_1 + p x_2, \tag{17}$$

where $f(z)$ is an arbitrary function of z, and the definition of $\boldsymbol{b}$ follows from Eq. (13),

$$\boldsymbol{b} = \left(\boldsymbol{R}^{\mathrm{T}} + p\boldsymbol{R}\right)\boldsymbol{a} = -p^{-1}\left(\boldsymbol{Q} + p\boldsymbol{R}\right)\boldsymbol{a}.$$

In order to diagonalize Eq. (15), the following eigenvalue problem is considered,

$$\boldsymbol{N}\boldsymbol{\xi} = p\boldsymbol{\xi}, \ \boldsymbol{\xi} = \left[\boldsymbol{a} \ \boldsymbol{b}\right]^{\mathrm{T}}. \tag{18}$$

A nontrivial solution of $\boldsymbol{\xi}$ exists if the determinant of the characteristic matrix according to Eq. (18) vanishes

$$\det\left(\boldsymbol{N} - p\boldsymbol{I}\right) = 0, \tag{19}$$

yielding twelve roots, i.e., eigenvalues p. The associated eigenvectors $\boldsymbol{\xi}$ are determined from Eq. (18). Due to the requirement that the strain energy must always be positive not depending on the kind of deformation, the eigenvalues p_s ($s = 1, 2, \ldots, 12$) of (19) are all complex and consist of six pairs of complex conjugates, as do their associated eigenvectors $\boldsymbol{a}_s$ and $\boldsymbol{b}_s$. Without loss in generality, we let

$$p_{\alpha+6} = \bar{p}_\alpha, \ \mathrm{Im}\ p_\alpha > 0, \ (\alpha = 1, 2, ..., 6), \tag{20}$$

$$\boldsymbol{a}_{\alpha+6} = \bar{\boldsymbol{a}}_\alpha, \ \boldsymbol{b}_{\alpha+6} = \bar{\boldsymbol{b}}_\alpha, \tag{21}$$

where Im stands for the imaginary part and the overbar denotes the complex conjugate. Assuming that all p_α are distinct, the general solution of $\boldsymbol{u}$ and $\boldsymbol{\varphi}$ is obtained from Eq. (17) by superposition of the independent eigensolutions associated with the p_α

$$\boldsymbol{u} = \boldsymbol{A}\boldsymbol{f}(z_\alpha) + \overline{\boldsymbol{A}\boldsymbol{f}(z_\alpha)}, \tag{22}$$

$$\boldsymbol{\varphi} = \boldsymbol{B}\boldsymbol{f}(z_\alpha) + \overline{\boldsymbol{B}\boldsymbol{f}(z_\alpha)}, \tag{23}$$

where the 6×6 complex matrices $\boldsymbol{A}$ and $\boldsymbol{B}$ and the 6×1 complex vector $\boldsymbol{f}$ are defined by

$$\begin{aligned} &\boldsymbol{A} = [\boldsymbol{a}_1, \boldsymbol{a}_2, \boldsymbol{a}_3, \boldsymbol{a}_4, \boldsymbol{a}_5, \boldsymbol{a}_6], \ \boldsymbol{B} = [\boldsymbol{b}_1, \boldsymbol{b}_2, \boldsymbol{b}_3, \boldsymbol{b}_4, \boldsymbol{b}_5, \boldsymbol{b}_6], \\ &\boldsymbol{f}(z_\alpha) = [f_1(z_1), f_2(z_2), f_3(z_3), f_4(z_4), f_5(z_5), f_6(z_6)]^{\mathrm{T}}, \ z_\alpha = x_1 + p_\alpha x_2. \end{aligned} \tag{24}$$

Up to here, 2D problems of QCs reduce to determining the unknown complex vector $\boldsymbol{f}$, which satisfies given boundary conditions. On the other hand, the determination of the constant matrices $\boldsymbol{A}$ and $\boldsymbol{B}$ and the eigenvalues p_α only depends on material properties, not on the boundary value problem itself.

It is noticed that the matrices $\boldsymbol{A}$ and $\boldsymbol{B}$ are nonsingular if the eigenvalues are distinct. However, they may be singular in some special cases in which eigenvalues coincide. Ting has undertaken extensive studies on these degenerate cases [38] which will not be discussed in detail here. In the following sections, we only consider configurations, where $\boldsymbol{A}$ and $\boldsymbol{B}$ are nonsingular. In addition, two matrices, $\boldsymbol{Y}$ and $\boldsymbol{H}$, used in the following analysis are defined by

$$\boldsymbol{Y} = \mathrm{i}\boldsymbol{A}\boldsymbol{B}^{-1}, \ \boldsymbol{H} = 2\mathrm{Re}\,\boldsymbol{Y}. \tag{25}$$

where $\mathrm{i} = \sqrt{-1}$. Following the proof for an elastic material [38] and a piezoelectric material [36], it can be shown that Matrix $\boldsymbol{Y}$ is a Hermitian matrix.

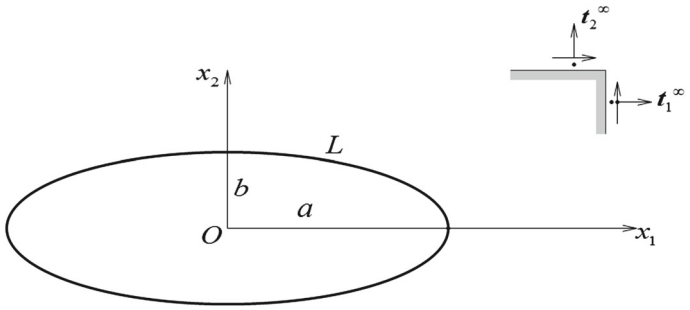

Fig. 1 An elliptical hole with remote uniform loading

4 An elliptic hole and a crack with uniform loading at infinity

The problem of determining stress distributions induced by holes has aroused considerable interest for almost half a century. Among various kinds of cavities, the elliptic shape and its geometric limits, i.e., circle and crack, have evoked the most interest among researchers. In an infinite anisotropic QC material, an elliptic hole is considered whose boundary L is mathematically described by

$$x_1 = a\cos\psi,\ x_2 = b\sin\psi, \tag{26}$$

where a and b are the half-lengths of the major and minor axes of the ellipse and ψ is a real parameter (Fig. 1). For an elliptic region, conformal mapping is the fundamental tool to transform the ellipse to a circle before solving the problem. The region (in the z_α-plane) is mapped onto the outside of the unit circle Γ (in the ζ_α-plane) by means of the function

$$z_\alpha = \frac{1}{2}\left[(a - \mathrm{i}p_\alpha b)\,\zeta_\alpha + (a + \mathrm{i}p_\alpha b)\,\zeta_\alpha^{-1}\right], \tag{27}$$

where the repeated Greek subscripts do not imply the summation convention. For a circle for which $a = b$, the mapping (27) is needed unless $p_\alpha = \mathrm{i}$. If the point $(x_1,\ x_2)$ is on the elliptic boundary L, Eq. (27) gives $\zeta_\alpha = \exp(\mathrm{i}\psi)$. For the region outside the ellipse, we obtain from Eq. (27)

$$\zeta_\alpha = \frac{z_\alpha + \sqrt{z_\alpha^2 - a^2 - p_\alpha^2 b^2}}{a - \mathrm{i}p_\alpha b}. \tag{28}$$

Thus, each point of the ellipse uniquely maps to the corresponding point on the unit circle Γ for any p_α. Thus, the mapping is one-to-one.

The elliptic hole is extended indefinitely in the x_3-direction, so the deformation is assumed to be 2D in the sense described in the previous section. The uniform loadings $\boldsymbol{t}_1^\infty = \left[\sigma_{11}^\infty, \sigma_{12}^\infty, \sigma_{13}^\infty, H_{11}^\infty, H_{12}^\infty, H_{13}^\infty\right]^{\mathrm{T}}$ and $\boldsymbol{t}_2^\infty = \left[\sigma_{21}^\infty, \sigma_{22}^\infty, \sigma_{23}^\infty, H_{21}^\infty, H_{22}^\infty, H_{23}^\infty\right]^{\mathrm{T}}$ are simultaneously applied at infinity. The associated strains $\boldsymbol{\varepsilon}_1^\infty$ and $\boldsymbol{\varepsilon}_2^\infty$ can be determined from the generalized Hooke's law in Eq. (1), so both the stress and strain applied at infinity are known.

By means of linear superposition, the generalized stress function vector $\boldsymbol{\varphi}$ of the boundary value problem can be rewritten as

$$\boldsymbol{\varphi} = x_1\boldsymbol{t}_2^\infty - x_2\boldsymbol{t}_1^\infty + \boldsymbol{B}\boldsymbol{f}(\zeta_\alpha) + \overline{\boldsymbol{B}\boldsymbol{f}(\zeta_\alpha)}, \tag{29}$$

The first part in Eq. (29) is the uniform stresses at infinity, and the second part is the perturbed solution due to the presence of the elliptic hole.

On the surface L_α of the cavity, the tractions vanish meaning that $\boldsymbol{\varphi} = \boldsymbol{0}$ on L_α. This leads to the relation

$$\boldsymbol{B}\boldsymbol{f}(s) + \bar{\boldsymbol{B}}\bar{\boldsymbol{f}}(s) = -\frac{1}{2}\left[a\left(s + s^{-1}\right)\boldsymbol{t}_2^\infty + \mathrm{i}b\left(s - s^{-1}\right)\boldsymbol{t}_1^\infty\right], \tag{30}$$

noting that on the cavity $\zeta = s = \exp(\mathrm{i}\psi)$ and

$$x_1(s) = \frac{1}{2}a\left(\frac{1}{s} + s\right),\ x_2(s) = \frac{1}{2}\mathrm{i}b\left(\frac{1}{s} - s\right). \tag{31}$$

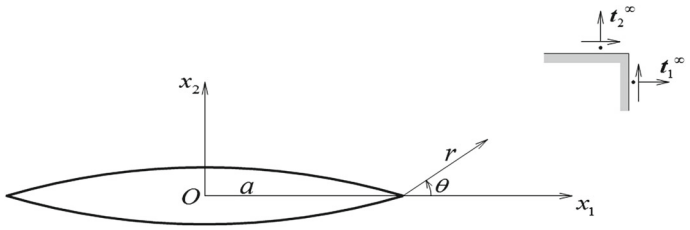

Fig. 2 A crack with remote uniform loading

Multiplying both sides of Eq. (30) by $\int_\Gamma \mathrm{d}s/(s-\zeta_\alpha)$ and then calculating the Cauchy integral leads to [24]

$$\boldsymbol{f}(\zeta_\alpha) = -\frac{1}{2}\left\langle \zeta_\alpha^{-1}\right\rangle \boldsymbol{B}^{-1}\left(a\boldsymbol{t}_2^\infty - \mathrm{i}b\boldsymbol{t}_1^\infty\right), \tag{32}$$

where $\left\langle \zeta_\alpha^{-1}\right\rangle$ is a diagonal matrix of ζ_α^{-1} with $\alpha = 1, 2, \ldots, 6$.

A finite straight crack is a special case of an elliptic hole where one of the axes becomes vanishingly small. With this understanding, the case of an arbitrarily oriented crack in a QC plane can be obtained by letting b approach zero (Fig. 2). Then, Eq. (32) reduces to

$$\boldsymbol{f}(z_\alpha) = -\frac{1}{2}\left\langle z_\alpha - \sqrt{z_\alpha^2 - a^2}\right\rangle \boldsymbol{B}^{-1}\boldsymbol{t}_2^\infty. \tag{33}$$

The full-field solutions for a crack subjected to uniform loading at infinity can be obtained by substituting Eq. (33) into Eqs. (22) and (29) and the latter into Eq. (12)

$$\boldsymbol{\sigma}_1 = \boldsymbol{t}_1^\infty + \mathrm{Re}\,\boldsymbol{B}\left\langle p_\alpha - \frac{p_\alpha z_\alpha}{\sqrt{z_\alpha^2 - a^2}}\right\rangle \boldsymbol{B}^{-1}\boldsymbol{t}_2^\infty,\ \boldsymbol{\sigma}_2 = \mathrm{Re}\,\boldsymbol{B}\left\langle \frac{z_\alpha}{\sqrt{z_\alpha^2 - a^2}}\right\rangle \boldsymbol{B}^{-1}\boldsymbol{t}_2^\infty, \tag{34}$$

$$\boldsymbol{u} = \mathrm{Re}\,\boldsymbol{A}\left\langle \sqrt{z_\alpha^2 - a^2} - z_\alpha\right\rangle \boldsymbol{B}^{-1}\boldsymbol{t}_2^\infty. \tag{35}$$

In the stresses, the homogeneous contribution of $\boldsymbol{t}_1^\infty$ has been added. In linear elastic fracture mechanics, the field intensity factors and the energy release rate are the two essential loading quantities. Approaching the crack tip $x_1 = a$, the field intensity factors are defined as

$$\boldsymbol{K} = \left[K_{\mathrm{II}}^{||}, K_{\mathrm{I}}^{||}, K_{\mathrm{III}}^{||}, K_{\mathrm{II}}^{\perp}, K_{\mathrm{I}}^{\perp}, K_{\mathrm{III}}^{\perp}\right]^{\mathrm{T}} = \lim_{x_1 \to a}\sqrt{2\pi\,(x_1 - a)}\sigma_2\,(x_1, \theta = 0)\,, \tag{36}$$

where the subscripts indicate the crack opening Modes I, II and III, and the superscripts $||$ and $\perp$ are associated with phonon and phason fields, respectively. Substituting Eq. (34) into Eq. (36), one obtains

$$\boldsymbol{K} = \sqrt{\pi a}\boldsymbol{t}_2^\infty. \tag{37}$$

which are independent of material constants only depending on the applied loading and the geometry of the body. The stress intensity factors can be regarded as a measure for the strength of the crack tip field.

In fracture mechanics, the crack tip field, i.e., the stresses and displacements close to a crack tip, is of fundamental importance. For this purpose, it is appropriate to introduce the polar coordinate system (r, θ) with its origin at the right crack tip (Fig. 2). The complex variables z_α are then replaced by

$$z_\alpha = a + r\,(\cos\theta + p_\alpha \sin\theta)\,. \tag{38}$$

The near-field solutions for the stresses and displacements are uniquely determined by the full-field solutions. Inserting Eq. (38) into Eqs. (34) and (35) and considering the limit $r \to 0$, we obtain

$$\begin{aligned}\boldsymbol{\sigma}_1\,(r,\theta) &= -\frac{1}{\sqrt{2\,\pi\,r}}\mathrm{Re}\,\boldsymbol{B}\left\langle \frac{p_\alpha}{\sqrt{\cos\theta + p_\alpha \sin\theta}}\right\rangle \boldsymbol{B}^{-1}\boldsymbol{K},\\ \boldsymbol{\sigma}_2\,(r,\theta) &= \frac{1}{\sqrt{2\,\pi\,r}}\mathrm{Re}\,\boldsymbol{B}\left\langle \frac{1}{\sqrt{\cos\theta + p_\alpha \sin\theta}}\right\rangle \boldsymbol{B}^{-1}\boldsymbol{K},\end{aligned} \tag{39}$$

$$\boldsymbol{u}\,(r,\theta) = \sqrt{\frac{2r}{\pi}}\mathrm{Re}\,\boldsymbol{A}\left\langle \sqrt{\cos\theta + p_\alpha \sin\theta}\right\rangle \boldsymbol{B}^{-1}\boldsymbol{K}. \tag{40}$$

From Eqs. (39) and (40), the mutual interdependence between phonon and phason quantities at the crack tip can be recognized. The crack tip fields are uniquely determined by Eqs. (39) and (40) if the stress intensity factors $\boldsymbol{K}$ are known. Vice versa, $\boldsymbol{K}$ can be determined from Eqs. (39) and (40) if the stresses or displacements close to the crack tip are known. The asymptotic distribution of the phonon and phason stress fields at the crack tip exhibits a singularity of the type $r^{-1/2}$. According to the generalized Hooke's law, Eq. (1), the strains have the same type of singularity. In contrast, the displacements show a behavior of the type $r^{1/2}$.

The crack opening displacement in the asymptotic near field is given by

$$\Delta \boldsymbol{u}\,(r,\pi) = \sqrt{\frac{2r}{\pi}}\boldsymbol{H}\boldsymbol{K}. \tag{41}$$

The crack opening tractions ahead of the crack tip in the plane $\theta = 0$ are given by

$$\boldsymbol{\sigma}_2\,(r,0) = \frac{1}{\sqrt{2\,\pi\,r}}\boldsymbol{K}. \tag{42}$$

It is noted that stresses in phonon and phason fields are uncoupled in this plane. In other words, the phonon loading alone cannot produce phason stress in the crack plane ahead of the crack tip and vice versa. Consequently, if the stress intensity factor is used to determine crack initiation and growth, the coupling field should have no effect. This leads us to conclude that single stress intensity factors are not suitable as a fracture criterion for QC materials.

Another possible fracture criterion for QC materials is based on the total energy release rate G. From the thermodynamic point of view, the total energy release rate is the most appropriate physical quantity to characterize the fracture behavior. It is defined as the change of the total potential energy Π of the cracked body related to an incremental growth of the crack area ΔA:

$$G = -\lim_{\Delta A\to 0}\frac{\Delta \Pi}{\Delta A} = -\frac{\mathrm{d}\Pi}{\mathrm{d}A}. \tag{43}$$

According to Irwin's crack closure integral, G equals the work performed by the stresses at the ligament of length Δa with the corresponding jumps of displacements $\Delta \boldsymbol{u}$ over the crack faces during a virtual crack closure process:

$$G = -\frac{\mathrm{d}\Pi}{\mathrm{d}A} = \lim_{\Delta a\to 0}\frac{1}{2\Delta a}\int_0^{\Delta a}\boldsymbol{\sigma}_2^{\mathrm{T}}\,(r,0)\,\Delta \boldsymbol{u}\,(\Delta a - r,\pi)\,\mathrm{d}r. \tag{44}$$

Equation (44) has a very clear physical meaning, that is, the total potential energy change associated with a crack advance Δa. Inserting Eqs. (41) and (42) into (44) and calculating the limiting value of the integral yield a relationship between the energy release rate and the stress intensity factors. This generalized Irwin's relationship is represented by the positive definite quadratic form

$$G = \frac{1}{4}\boldsymbol{K}^{\mathrm{T}}\boldsymbol{H}\boldsymbol{K}. \tag{45}$$

The total energy release rate is determined by a unique quantity in which phonon and phason fields are coupled, even if the phason stress intensity factor is zero. In our previous work [9], numerical results for a Griffith crack with σ_{22}^{∞} or σ_{12}^{∞} applied at infinity have been illustrated to visualize the influence of the phason field on G. This shows that the phason field strongly influences the fracture behavior of the material, and reveals the physical significance of the results relative to the phason and the difference between the mechanical behaviors of crack problems in crystals and QCs. The existence of the phason field and the coupling between phonon and phason fields induce an increment of G and thus increase the loading of a Mode II crack, but result in the opposite effect for a Mode I crack.

5 Stress intensity factors for point forces at arbitrary locations and crack weight functions

For many geometrical configurations, the stress intensity factors for particular loadings are known from handbooks. Many methods exist to determine stress intensity factors for specific loading conditions. Here, different techniques of linear elasticity applied to the determination of stresses and deformations play a fundamental role. Crack weight functions, which are frequently also called influence functions, are representing a very powerful tool to obtain stress intensity factors for a given geometry exposed to arbitrary loading applying the principle of linear superposition. They relate the stress intensity factors in a cracked elastic body to point forces at arbitrary locations. Thus, the influence functions can be interpreted as Green's functions for stress intensity factors.

Crack weight functions were introduced by Bueckner [3], and the theory was further developed by Rice [29]. The weight function theory for cracks was later extended toward 3D boundary value problems, for instance planar cracks with curved fronts, or crack interaction with inhomogeneities such as particles and dislocations. A comprehensive theory and review of earlier work were given by Rice [30]. The concept of crack weight functions has also been extended to piezoelectric materials [22,23].

For a QC material, the theory has to be extended including a point phason force and the phason stress intensity factors. We consider a combined problem as illustrated in Fig. 3. It consists of uniform loadings $\boldsymbol{t}_1^{\infty}$ and $\boldsymbol{t}_2^{\infty}$ at infinity (subproblem 1) and the point forces $\boldsymbol{F} = [P_1, P_2, P_3, Q_1, Q_2, Q_3]^{\mathrm{T}}$ which collocate point phonon and point phason forces P_i and Q_i at $\boldsymbol{x} = (r\cos\theta, r\sin\theta)^{\mathrm{T}}$ (subproblem 2). For plane problems, $\boldsymbol{F}$ have the dimension of line forces. According to the linear superposition principle, the field intensity factors are

$$\boldsymbol{K} = \boldsymbol{K}^1 + \boldsymbol{K}^2, \tag{46}$$

where $\boldsymbol{K}^1$ are given in Eq. (37), and $\boldsymbol{K}^2$ are the field intensity factors due to the point forces of the subproblem 2,

$$\boldsymbol{K}^2 = \boldsymbol{h}\boldsymbol{F}, \tag{47}$$

where the term $\boldsymbol{h}(\boldsymbol{x}, a)$ is a 6×6 matrix containing the weight functions to be formulated. They weight the prescribed forces $\boldsymbol{F}$ to determine the related stress intensity factors. Due to the presence of $\boldsymbol{t}_1^{\infty}$, $\boldsymbol{t}_2^{\infty}$ and $\boldsymbol{F}$, the remote displacements $\boldsymbol{u}^{\infty}$ and the displacements $\boldsymbol{u}(\boldsymbol{x})$ at $\boldsymbol{x}$ become

$$\boldsymbol{u}^{\infty} = \boldsymbol{C}^1\boldsymbol{t}_2^{\infty} + \boldsymbol{C}^{12}\boldsymbol{F},\ \boldsymbol{u}\,(\boldsymbol{x}) = \boldsymbol{C}^{21}\boldsymbol{t}_2^{\infty} + \boldsymbol{C}^2\boldsymbol{F}, \tag{48}$$

where $\boldsymbol{C}^1$ and $\boldsymbol{C}^2$ are the symmetric generalized compliance matrices of the subproblems 1 and 2, respectively. $\boldsymbol{C}^{12} = \boldsymbol{C}^{21}$ are the generalized cross-compliance matrices of both subproblems, which are identical according to Betti's theorem of reciprocity. The total potential energy Π for the combined problem is defined as the difference between the internal strain energy U stored inside the cracked body and the generalized work done by both loadings,

$$\Pi\left(\boldsymbol{t}_2^{\infty}, \boldsymbol{F}, a\right) = U - \boldsymbol{t}_2^{\infty}\boldsymbol{u}^{\infty}\mathrm{d}S - \boldsymbol{F}\boldsymbol{u}. \tag{49}$$

The infinitesimal area $\mathrm{d}S$ is the one the stress vector $\boldsymbol{t}_2^{\infty}$ is related to. In addition, the following partial derivatives are satisfied

$$u_I^{\infty} = -\frac{\partial\Pi\left(t_{2I}^{\infty}, F_I, a\right)}{\partial t_{2I}^{\infty}},\ u_I\,(\boldsymbol{x}) = -\frac{\partial\Pi\left(t_{2I}^{\infty}, F_I, a\right)}{\partial F_I}. \tag{50}$$

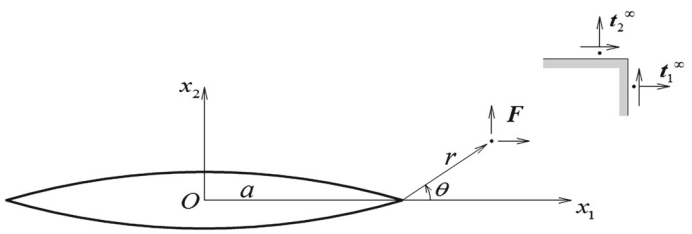

Fig. 3 A crack with remote uniform loading and point forces

Here, the matrix notation has been switched to the index notation. For a plane problem, the total potential energy is related to the unit thickness, and thus, the energy release rate defined in Eq. (43) reads

$$G\left(t_{2I}^{\infty}, F_I, a\right) = -\frac{1}{2}\frac{\partial \Pi\left(t_{2I}^{\infty}, F_I, a\right)}{\partial a} \tag{51}$$

with the total length of a central crack $\ell = 2a$. Differentiation of Eqs. (50) and (51) leads to

$$\frac{\partial G}{\partial F_I} = \frac{1}{2}\frac{\partial u_I(\boldsymbol{x})}{\partial a}. \tag{52}$$

Applying the generalized Irwin's relationship according to Eq. (45), the energy release rate is related to the field intensity factors of the combined problem. Taking into account Eqs. (46) and (47) gives

$$\boldsymbol{G} = \frac{1}{4}\left(\sqrt{\pi a}\boldsymbol{t}_2^{\infty} + \boldsymbol{h}\boldsymbol{F}\right)^{\mathrm{T}}\boldsymbol{H}\left(\sqrt{\pi a}\boldsymbol{t}_2^{\infty} + \boldsymbol{h}\boldsymbol{F}\right). \tag{53}$$

Differentiating Eq. (53) with respect to F_I as well as Eq. (48) with respect to a and then substituting both into Eq. (52) provide

$$\left(\sqrt{\pi a}\boldsymbol{t}_2^{\infty} + \boldsymbol{h}\boldsymbol{F}\right)^{\mathrm{T}}\boldsymbol{H}\cdot\boldsymbol{h} = \frac{\mathrm{d}\boldsymbol{C}^{12}}{\mathrm{d}a}\boldsymbol{t}_2^{\infty} + \frac{\mathrm{d}\boldsymbol{C}^{2}}{\mathrm{d}a}\boldsymbol{F}. \tag{54}$$

Since the weight functions are a property of the geometry of the boundary value problem and are independent of specific loading conditions, we can choose $\boldsymbol{F}$ to be zero. Then, Eq. (54) reduces to

$$\boldsymbol{h} = \frac{1}{\sqrt{\pi a}}\boldsymbol{H}^{-1}\frac{\mathrm{d}\boldsymbol{C}^{12}}{\mathrm{d}a}. \tag{55}$$

Comparing Eqs. (35) and Eq. (48), it is obvious that for $\boldsymbol{F} = \boldsymbol{0}$

$$\boldsymbol{C}^{12} = \mathrm{Re}\,\boldsymbol{A}\left\langle\sqrt{z_\alpha^2 - a^2} - z_\alpha\right\rangle\boldsymbol{B}^{-1}. \tag{56}$$

The derivative with respect to a has to be performed in a crack tip coordinate system accounting for the transformation $\hat{x}_1 = x_1 + a$. The origin of $\hat{x}_1$ is at the left crack tip. Substituting Eq. (56) into Eq. (55) leads to the weight functions for the crack in an infinite domain with point forces $\boldsymbol{F}$:

$$\boldsymbol{h} = \frac{-1}{\sqrt{\pi a}}\boldsymbol{H}^{-1}\mathrm{Re}\,\boldsymbol{A}\left\langle\frac{\sqrt{z_\alpha + a}}{\sqrt{z_\alpha - a}}\right\rangle\boldsymbol{B}^{-1}. \tag{57}$$

For point loads applied on the right crack surfaces ($x_1 > 0$), where $z_\alpha = x_1$, the weight functions become

$$\boldsymbol{h} = \pm\frac{-1}{\sqrt{\pi a}}\boldsymbol{H}^{-1}\sqrt{\frac{a + x_1}{a - x_1}}\mathrm{Re}\left(-\mathrm{i}\boldsymbol{A}\boldsymbol{B}^{-1}\right) = \pm\frac{1}{2\sqrt{\pi a}}\sqrt{\frac{a + x_1}{a - x_1}}\boldsymbol{I}, \tag{58}$$

where the positive and negative signs are related to the upper and lower crack surfaces, respectively. The unit tensor $\boldsymbol{I}$ is introduced accounting for Eq. (25).

The crack tip weight functions are of interest, since fields close to the crack tip have a major influence on the fracture quantities. In the polar coordinate system (r, θ), the crack tip weight functions are obtained from Eq. (57)

$$\boldsymbol{h} = -\sqrt{\frac{2}{\pi r}}\boldsymbol{H}^{-1}\mathrm{Re}\,\boldsymbol{A}\left\langle\frac{1}{\sqrt{\cos\theta + p_\alpha\sin\theta}}\right\rangle\boldsymbol{B}^{-1}. \tag{59}$$

For the crack surfaces at the right crack tip, a similar treatment as with Eq. (58) leads to the near-tip weight functions

$$\boldsymbol{h} = \pm\frac{1}{\sqrt{2\pi r}}\boldsymbol{I}. \tag{60}$$

Concerning stress intensity factors, each arbitrary loading configuration can be constructed by point loads on the crack faces, following the principle of linear superposition. By integrating the weight functions together with prescribed loads along the Neumann boundaries, Eq. (58) can therefore be used to calculate stress intensity factors for arbitrary distributed loadings, too. The advantage of using weight functions is that once they have been obtained for a given cracked geometry from a known displacement solution for a reference loading, the stress intensity factors at the same geometry can be determined for any kind of loading. The weight function method can also be efficiently applied within the context of numerical methods, e.g., finite element or boundary element techniques.

6 Numerical calculation of crack weight functions

Now, the numerical calculation of crack weight functions based on the theory derived above is presented. For icosahedral QCs, there are five independent elastic constants: two for C_{ijkl}, two for K_{ijkl} and one for R_{ijkl}. The phonon elastic constants are represented by the general notation for isotropic elastic materials:

$$C_{ijkl} = \lambda\delta_{ij}\delta_{kl} + \mu\left(\delta_{ik}\delta_{jl} + \delta_{il}\delta_{jk}\right),$$

where λ and μ are the Lamé constants and δ_{ij} is the Kronecker unit tensor. The coordinate system is now chosen with the x_3-axis pointing toward a vertex of an icosahedral QC [5]. Considering properties of symmetry outlined in Eq. (2), K_{ijkl} and R_{ijkl}, arranged as $ij, kl = 11, 22, 33, 23, 31, 12, 32, 13, 21$, have the following matrix form

$$[K] = \begin{bmatrix} K_1 & 0 & 0 & 0 & K_2 & 0 & 0 & K_2 & 0 \\ 0 & K_1 & 0 & 0 & -K_2 & 0 & 0 & K_2 & 0 \\ 0 & 0 & K_2+K_1 & 0 & 0 & 0 & 0 & 0 & 0 \\ 0 & 0 & 0 & K_1-K_2 & 0 & K_2 & 0 & 0 & -K_2 \\ K_2 & -K_2 & 0 & 0 & K_1-K_2 & 0 & 0 & 0 & 0 \\ 0 & 0 & 0 & K_2 & 0 & K_1 & -K_2 & 0 & 0 \\ 0 & 0 & 0 & 0 & 0 & -K_2 & K_1-K_2 & 0 & -K_2 \\ K_2 & K_2 & 0 & 0 & 0 & 0 & 0 & K_1-K_2 & 0 \\ 0 & 0 & 0 & -K_2 & 0 & 0 & -K_2 & 0 & K_1 \end{bmatrix}$$

$$[R] = R\begin{bmatrix} 1 & 1 & 1 & 0 & 0 & 0 & 0 & 1 & 0 \\ -1 & -1 & 1 & 0 & 0 & 0 & 0 & -1 & 0 \\ 0 & 0 & -2 & 0 & 0 & 0 & 0 & 0 & 0 \\ 0 & 0 & 0 & 0 & 0 & -1 & 1 & 0 & -1 \\ 1 & -1 & 0 & 0 & 1 & 0 & 0 & 0 & 0 \\ 0 & 0 & 0 & -1 & 0 & -1 & 0 & 0 & 1 \\ 0 & 0 & 0 & 0 & 0 & -1 & 1 & 0 & -1 \\ 1 & -1 & 0 & 0 & 1 & 0 & 0 & 0 & 0 \\ 0 & 0 & 0 & -1 & 0 & -1 & 0 & 0 & 1 \end{bmatrix}.$$

It is obvious that the material constants λ, μ, K_1, K_2 and R, which are experimentally measured by various methods, e.g., X-ray diffraction, neutron scattering, etc., are very important for stress analyses of icosahedral QCs. For the most important icosahedral Al-Pd-Mn QC, we take the data of elastic moduli as [15,37]

$$\lambda = 74.9\,\text{GPa},\ \mu = 72.4\,\text{GPa},\ K_1 = 0.043\,\text{GPa},\ K_2 = -0.022\,\text{GPa},\ R = 0.215\,\text{GPa}.$$

The distinct eigenvalues are

$$\begin{aligned} &p_1 = -0.479226 + 1.04008i,\ p_2 = 0.479226 + 1.04008i, \\ &p_3 = -0.189449 + 0.665282i,\ p_4 = 0.189449 + 0.665282i, \\ &p_5 = 1.595648i,\ p_6 = i. \end{aligned}$$

To compare results calculated for classical elastic materials to those from Eq. (59), we consider a special case, i.e., the icosahedral QC material reduces to an isotropic elastic material. In this case, no phonon–phason field coupling effect is taken into account, i.e., $R = 0$. Thus, the crack tip weight functions $\boldsymbol{h}_{\mathrm{I}}^{ie}$ for isotropic elastic materials associated with a Mode I crack opening with the following form [3,29]

$$\boldsymbol{h}_{\mathrm{I}}^{ie} = \frac{1}{2\sqrt{2\pi r}\,(1-\nu)}\begin{bmatrix} \cos\frac{\theta}{2}\left(2\nu - 1 + \sin\frac{\theta}{2}\sin\frac{3\theta}{2}\right) \\ \sin\frac{\theta}{2}\left(2 - 2\nu - \cos\frac{\theta}{2}\cos\frac{3\theta}{2}\right) \end{bmatrix}. \tag{61}$$

Figures 4, 5, 6 show all six stress intensity factors for a Griffith crack in Al-Pd-Mn QC, which have been calculated using the crack tip weight functions according to Eq. (59). The dotted graph represents K_{I}^{ie} for the isotropic elastic body with $\nu = 0.254$, which is calculated from Eq. (61). A near-tip line force P_i, $i = 1, 2, 3$ of magnitude 1 N/m is orientated into the x_1-, x_2- or x_3-direction, respectively. Its position is defined by the angle θ and a distance $r = 10^{-3}$ m from the crack tip, see Fig. 3.

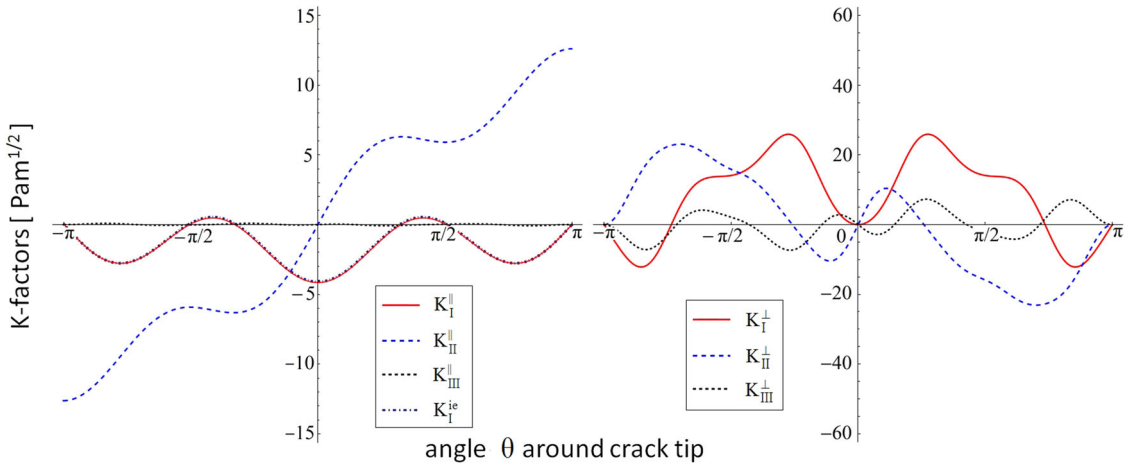

Fig. 4 Stress intensity factors (*left* phonon, *right* phason) for a Griffith crack due to line force P_1 at $r = 10^{-3}$ m and angle θ around the crack tip

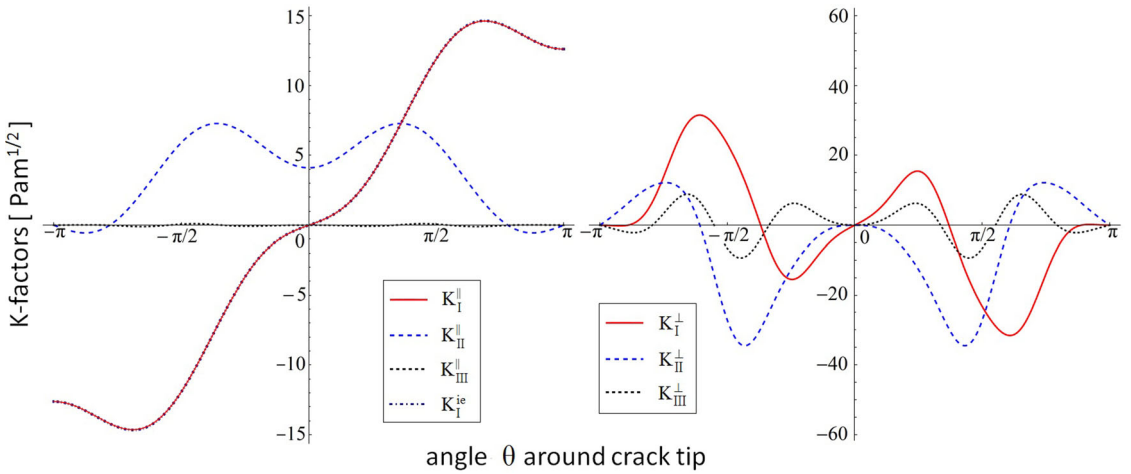

Fig. 5 Stress intensity factors (*left* phonon, *right* phason) for a Griffith crack due to line force P_2 at $r = 10^{-3}$ m and angle θ around the crack tip

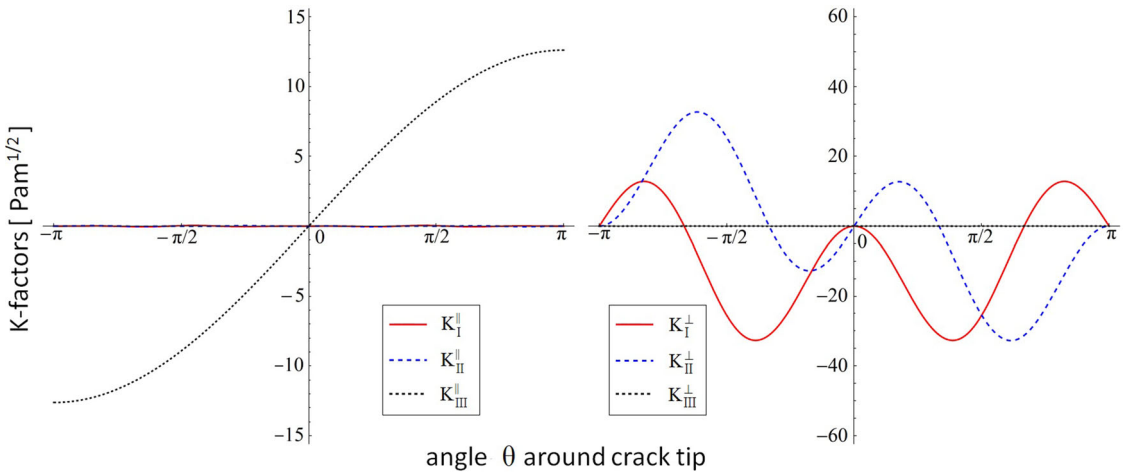

Fig. 6 Stress intensity factors (*left* phonon, *right* phason) for a Griffith crack due to line force P_3 at $r = 10^{-3}$ m and angle θ around the crack tip

Like in piezoelectric fracture mechanics [23], the intensity factors for the different types of fields are independent from each other, which is due to the decoupling of phonon and phason stresses in front of the crack tip. However, at arbitrary locations around the crack, there is a coupling of phonon loading and phason stresses and displacements and vice versa. The results in Figs. 1 and 2 show that the phonon intensity factor $K_{\mathrm{III}}^{||}$ is zero for all angles θ. However, the results in Fig. 3 show that the line load P_3 only produces a nonzero phonon intensity factor $K_{\mathrm{III}}^{||}$, whereas the phason stress intensity factors exhibit nonzero $K_{\mathrm{I}}^{\perp}$ and $K_{\mathrm{II}}^{\perp}$ but a vanishing $K_{\mathrm{III}}^{\perp}$. On the other hand, a Mode I/II loading (Figs. 4, 5) produces a finite $K_{\mathrm{III}}^{\perp}$ at the phason field. Comparing K_{I} for the classical isotropic body and the icosahedral QC, the results of the phonon field are very close to those for the isotropic elastic material with a maximum deviation of 6.8 % due to P_1 and only 0.18 % due to P_2.

7 Conclusions

In the present work, we treat the generalized 2D problem of an elliptic hole and a crack in an infinite 3D QC medium subjected to uniform phonon loading together with uniform phason loading at infinity. The analysis is based on the generalized Stroh formalism and the exact boundary conditions at the rim of the hole. Finally, the explicit solutions for the coupled fields, which are very convenient to be used studying dislocations, cracks and inhomogeneities in the new solid phase, are provided in a closed form.

Reducing the elliptic hole to a crack, the analytical expressions for both the entire fields and the asymptotic fields near the crack tip are determined. The results show that the distribution of the phonon field is similar to the corresponding results in conventional linear elastic fracture mechanics, while the phason field, which arises from the coupling relationship between the phonon and the phason fields, is particular for QCs but also exhibits the square root singularity around the crack tip.

The field intensity factors are independent of material constants. The principles of the Griffith–Irwin linear elastic fracture mechanics for conventional materials still hold for QC materials, except the determination of the field intensity factors due to the presence of the phason field. Additionally, the crack strain energy release rate is given, which is different from its counterpart in conventional linear elastic fracture mechanics. The results show that the existence of the phason field and the coupling between phonon and phason fields strongly affects the configuration and strain energy of the crack.

The weight functions for cracks in QC materials provide a novel way to yield the field intensity factors due to applied loadings at arbitrary locations. The weight functions are formulated from the total potential energy for the combined problem with coupled displacements as dependent variables and the applied loadings as independent variables. Applying the principle of linear superposition and Betti's theorem of reciprocity, the weight functions are derived for the different crack opening Modes from any known mixed-mode solution in terms of displacements of the cracked body under specific coupled loads. Results are presented for cracks being exposed to a loading by near-tip line forces. The classical decoupling of the in-plane Modes I and II on the one hand and Mode III on the other is only manifested in the phonon stress intensity factors. In the phason, $K_{\mathrm{III}}^{\perp}$ is evoked by in-plane loading and vanishes for an out-of-plane line force.

Although tools have been provided to calculate the energy release rate and stress intensity factors for QCs, it is still an open question how these loading quantities have to be interpreted within the context of a fracture criterion. This is certainly one of the most essential and challenging research topics in the field of fracture mechanics of QCs for the near future.

Acknowledgments The authors are very grateful to the anonymous reviewers for their helpful suggestions. The work is supported by the National Natural Science Foundation of China (No. 11172319), Chinese Universities Scientific Fund (Nos. 2011JS046 and 2013BH008), Opening Fund of State Key Laboratory of Nonlinear Mechanics, Program for New Century Excellent Talents in University (No. NCET-13-0552), National Science Foundation for postdoctoral Scientists of China (No. 2013M541086) and the Alexander von Humboldt Foundation in Germany.

References

1. Athanasiou, N.S., Politis, C., Spirlet, J.C., Baskoutas, S., Kapaklis, V.: The significance of valence electron concentration on the formation mechanism of some ternary aluminum-based quasicrystals. Int. J. Mod. Phys. B **16**(31), 4665–4683 (2002)
2. Barnett, D.M., Lothe, J.: Line force loadings on anisotropic half-spaces and wedges. Phys. Norv. **8**, 13–22 (1975)
3. Bueckner, H.F.: Novel principle for the computation of stress intensity factors. Z. Angew. Math. Mech. **50**, 529–546 (1970)

4. Dai, M.X., Urban, K.: Twins in icosahedral Al-Cu-Fe. Philos. Mag. Lett. **67**(2), 67–71 (1993)
5. Ding, D.H., Yang, W.G., Hu, C.Z., Wang, R.H.: Generalized elasticity theory of quasicrystals. Phys. Rev. B **48**(10), 7003–7010 (1993)
6. Ebert, P., Feuerbacher, M., Tamura, N., Wollgarten, M., Urban, K.: Evidence for a cluster-based structure of AlPdMn single quasicrystals. Phys. Rev. Lett. **77**(18), 3827–3830 (1996)
7. Fan, T.Y., Mai, Y.W.: Elasticity theory, fracture mechanics, and some relevant thermal properties of quasi-crystalline materials. Appl. Mech. Rev. **57**, 325–343 (2004)
8. Gao, Y., Ricoeur, A.: Three-dimensional analysis of a spheroidal inclusion in a two-dimensional quasicrystal body. Philos. Mag. **92**(34), 4334–4353 (2012)
9. Gao, Y., Ricoeur, A., Zhang, L.: Plane problems of cubic quasicrystal media with an elliptic hole or a crack. Phys. Lett. A **375**, 2775–2781 (2011)
10. Gao, Y., Zhao, B.S.: General solutions of three-dimensional problems for two-dimensional quasicrystals. Appl. Math. Model. **33**(8), 3382–3391 (2009)
11. Gao, Y., Zhao, Y.T., Zhao, B.S.: Boundary value problems of holomorphic vector functions in 1D QCs. Phys. B **394**(1), 56–61 (2007)
12. Hu, C.Z., Wang, R.H., Ding, D.H.: Symmetry groups, physical property tensors, elasticity and dislocations in quasicrystals. Rep. Prog. Phys. **63**(1), 1–39 (2000)
13. Hu, C.Z., Wang, R.H., Yang, W.G., Ding, D.H.: Point groups and elastic properties of two-dimensional quasicrystals. Acta Crystallogr. Sect. A **52**, 251–256 (1996)
14. Hwu, C.: Thermal stresses in an anisotropic plate disturbed by an insulated elliptic hole or crack. ASME J. Appl. Mech. **57**(4), 916–922 (1990)
15. Letoublon, A., De Boissieu, M., Boudard, M., Mancini, L., Gastaldi, J., Hennion, B., Caudron, R., Bellissent, R.: Phason elastic constants of the icosahedral Al-Pd-Mn phase derived from diffuse scattering measurements. Philos. Mag. Lett. **81**(4), 273–283 (2001)
16. Levine, D., Lubensky, T.C., Ostlund, S., Ramaswamy, S., Steinhardt, P.J., Toner, J.: Elasticity and dislocations in pentagonal and icosahedral quasicrystals. Phys. Rev. Lett. **54**(14), 1520–1523 (1985)
17. Levine, D., Steinhardt, P.J.: Quasi-crystals: a new class of ordered structure. Phys. Rev. Lett. **53**(26), 2477–2480 (1984)
18. Levine, D., Steinhardt, P.J.: Quasicrystals. 1. Definition and structure. Phys. Rev. B **34**(2), 596–616 (1986)
19. Li, X.F., Fan, T.Y.: New method for solving elasticity problems of some planar quasicrystals and solutions. Chin. Phys. Lett. **15**, 278–280 (1998)
20. Li, X.F., Fan, T.Y., Sun, Y.F.: A decagonal quasicrystal with a Griffith crack. Philos. Mag. A **79**, 1942–1953 (1999)
21. Lubensky, T.C., Ramaswamy, S., Joner, J.: Hydrodynamics of icosahedral quasicrystals. Phys. Rev. B **32**(11), 7444–7452 (1985)
22. Ma, L.F., Chen, Y.H.: Weight functions for interface cracks in dissimilar anisotropic piezoelectric materials. Int. J. Fract. **110**(3), 263–279 (2001)
23. McMeeking, R., Ricoeur, A.: The weight function for cracks in piezoelectrics. Int. J. Solids Struct. **40**(22), 6143–6162 (2003)
24. Muskhelishvili, N.I.: Some Basic Problems of the Mathematical Theory of Elasticity. Noordhoff, Groningen (1953)
25. Pak, Y.E.: Crack extension force in a piezoelectric material. ASME J. Appl. Mech. **57**, 647–653 (1990)
26. Park, J.Y., Ogletree, D.F., Salmeron, M., Ribeiro, R.A., Canfield, P.C., Jenks, C.J., Thiel, P.A.: High frictional anisotropy of periodic and aperiodic directions on a quasicrystal surface. Science **309**(5739), 1354–1356 (2005)
27. Park, J.Y., Sacha, G.M., Enachescu, M., Ogletree, D.F., Ribeiro, R.A., Canfield, P.C., Jenks, C.J., Thiel, P.A., Saenz, J.J., Salmeron, M.: Sensing dipole fields at atomic steps with combined scanning tunneling and force microscopy. Phys. Rev. Lett. **95**(13), 136802 (2005)
28. Peng, Y.Z., Fan, T.Y.: Perturbation method solving elastic problems of icosahedral quasicrystals containing a circular crack. Chin. Phys. **9**, 764–766 (2000)
29. Rice, J.R.: Some remarks on elastic crack-tip stress fields. Int. J. Solids Struct. **8**, 751–758 (1972)
30. Rice, J.R.: Weight function theory for three-dimensional elastic crack analysis. In: Wei, R.P., Gangloff, R.P. (eds.) Fracture Mechanics: Perspectives and Directions (Twentieth Symposium). American Society for Testing and Materials, Philadelphia, pp. 29–57 (1989)
31. Shechtman, D., Blech, I., Gratias, D., Cahn, J.W.: Metallic phase with long-range orientational order and no translational symmetry. Phys. Rev. Lett. **53**(20), 1951–1953 (1984)
32. Socolar, J.E.S.: Simple octagonal and dodecagonal quasicrystals. Phys. Rev. B **39**(15), 10519–10551 (1989)
33. Stadnik, Z.: Physical Properties of Quasicrystals, vol. 126. Springer, Berlin (1999)
34. Stroh, A.N.: Dislocations and cracks in anisotropic elasticity. Philos. Mag. **3**, 625–646 (1958)
35. Stroh, A.N.: Steady state problems in anisotropic elasticity. J. Math. Phys. **41**, 77–103 (1962)
36. Suo, Z., Kuo, C.M., Barnett, D.M., Willis, J.R.: Fracture mechanics for piezoelectric ceramics. J. Mech. Phys. Solids **40**(4), 739–765 (1992)
37. Tanaka, K., Mitarai, Y., Koiwa, M.: Elastic constants of Al-based icosahedral quasicrystals. Philos. Mag. A **73**(6), 1715–1723 (1996)
38. Ting, T.C.T.: Anisotropic Elasticity: Theory and Applications. Oxford University Press, Oxford (1996)
39. Ting, T.C.T.: Recent developments in anisotropic elasticity. Int. J. Solids Struct. **37**(1–2), 401–409 (2000)
40. Wollgarten, M., Beyss, M., Urban, K., Liebertz, H., Koster, U.: Direct evidence for plastic deformation of quasicrystals by means of a dislocation mechanism. Phys. Rev. Lett. **71**(4), 549–552 (1993)
41. Zhou, W.M., Fan, T.Y.: Plane elasticity problem of two-dimensional octagonal quasicrystals and crack problem. Chin. Phys. **10**, 743–747 (2001)
42. Zhu, A.Y., Fan, T.Y.: Elastic analysis of a mode II crack in an icosahedral quasicrystal. Chin. Phys. **16**(4), 1111–1118 (2007)